Published Ahead of Print on September 11, 2019 as 10.1212/WNL.0000000000008315

ARTICLE

Amyloid and cerebrovascular burden divergently influence brain functional network changes over time

Joanna Su Xian Chong, PhD,* Hyemin Jang, MD,* Hee Jin Kim, MD, PhD, Kwun Kei Ng, PhD, Duk L. Na, MD, PhD, Jae Hong Lee, MD, PhD, Sang Won Seo, MD, PhD,‡ and Juan Zhou, PhD‡

Neurology® 2019;93:1-12. doi:10.1212/WNL.0000000000008315

Correspondence
Dr. Zhou
helen.zhou@duke-nus.edu.sg
or Dr. Seo
sangwonseo@empal.com

Abstract

Objective

To examine the effects of baseline Alzheimer disease and cerebrovascular disease markers on longitudinal default mode network (DMN) and executive control network (ECN) functional connectivity (FC) changes in mild cognitive impairment (MCI).

Methods

We studied 30 patients with amnestic MCI (aMCI) and 55 patients with subcortical vascular MCI (svMCI) with baseline Pittsburgh Compound B (PiB)–PET scans and longitudinal MRI scans. Participants were followed up clinically with annual MRI for up to 4 years (aMCI: 26 with 2 timepoints, 4 with 3 timepoints; svMCI: 13 with 2 timepoints, 16 with 3 timepoints, 26 with 4 timepoints).

Results

β-Amyloid (Aβ) burden was associated with longitudinal DMN FC declines, while cerebrovascular burden was associated with longitudinal ECN FC changes. When patients were divided into PiB+ and PiB− groups, PiB+ patients showed longitudinal DMN FC declines, while patients with svMCI showed longitudinal ECN FC increases. Direct comparisons between the 2 groups without mixed pathology (aMCI PiB+ and svMCI PiB−) recapitulated this divergent pattern: aMCI PiB+ patients showed steeper longitudinal DMN FC declines, while svMCI PiB− patients showed steeper longitudinal ECN FC increases. Finally, using baseline PiB uptake and lacune numbers as continuous variables, baseline PiB uptake showed inverse U-shape associations with longitudinal DMN FC changes in both MCI subtypes, while baseline lacune numbers showed mainly inverse U-shape relationships with longitudinal ECN FC changes in patients with svMCI.

Conclusions

Our findings underscore the divergent effects of Aβ and cerebrovascular burden on longitudinal FC changes in the DMN and ECN in the predementia stage, which reflect the underlying pathology and may be used to track early changes in Alzheimer disease and cerebrovascular disease.

*These authors contributed equally to this work as co–first authors.

‡These authors contributed equally to this work as co–senior authors.

From the Centre for Cognitive Neuroscience (J.S.X.C., K.K.N., J.Z.), Neuroscience and Behavioural Disorders Programme, Duke-National University of Singapore Medical School; Department of Neurology (H.J., H.J.K., D.L.N., S.W.S.), Samsung Medical Center, Sungkyunkwan University School of Medicine; Department of Neurology (J.H.L.), Asan Medical Center, Ulsan University School of Medicine, Seoul, Korea; and Clinical Imaging Research Centre, National University of Singapore (J.Z.).

Go to Neurology.org/N for full disclosures. Funding information and disclosures deemed relevant by the authors, if any, are provided at the end of the article.

Glossary

Aβ = β-amyloid; **AD** = Alzheimer disease; **ADL** = activities of daily living; **aMCI** = amnestic mild cognitive impairment; **DMN** = default mode network; **ECN** = executive control network; **FC** = functional connectivity; **FLAIR** = fluid-attenuated inversion recovery; **GMV** = gray matter volume; **MCI** = mild cognitive impairment; **MNI** = Montreal Neurological Institute; **PiB** = Pittsburgh compound B; **SNSB** = Seoul Neuropsychological Screening Battery; **SUVR** = standardized uptake value ratio; **svMCI** = subcortical vascular mild cognitive impairment; **VOI** = volume of interest.

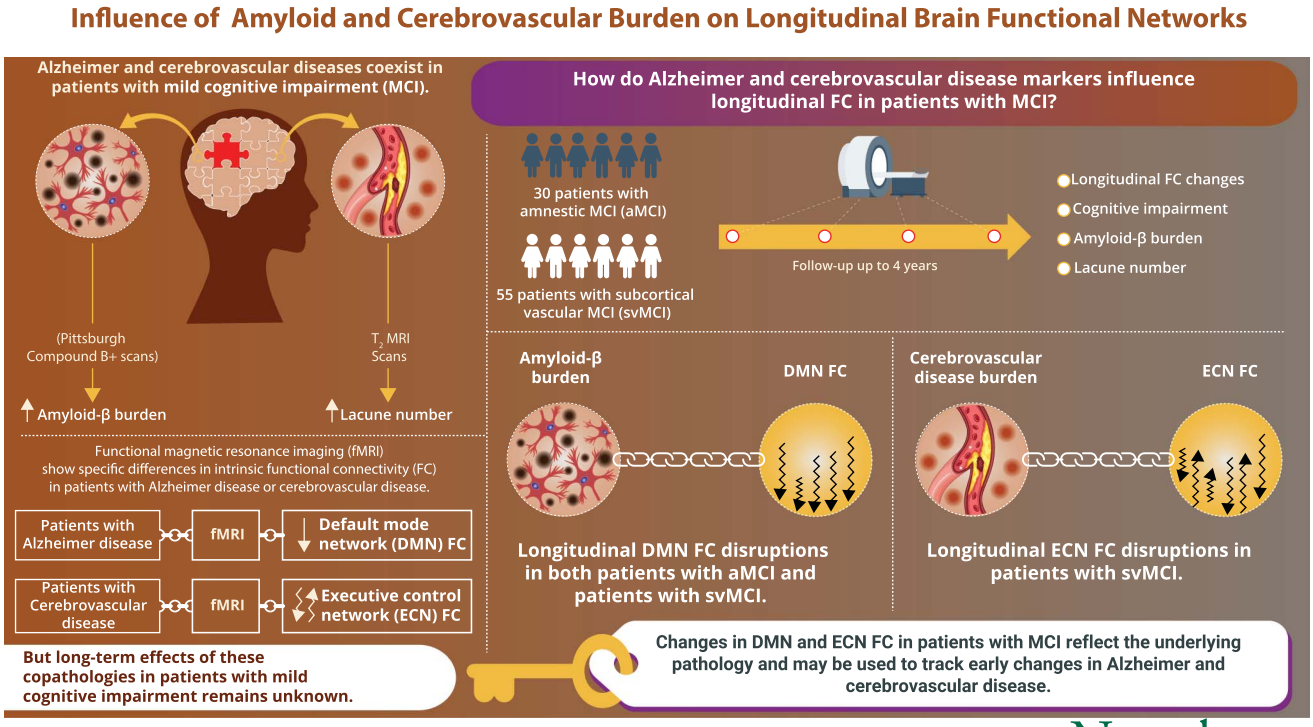

doi:10.1212/WNL.0000000000008315

Neurology®

Alzheimer disease (AD) and subcortical vascular dementia are among the most common causes of late-life cognitive impairment. AD is characterized by memory dysfunction and the presence of β-amyloid (Aβ) plaques and neurofibrillary tau tangles, while subcortical vascular dementia features extensive cerebrovascular disease and frontal-executive dysfunction.[1] Aβ deposition and cerebrovascular disease commonly coexist in patients with cognitive impairment, and evidence from autopsy and neuroimaging studies suggests that these 2 pathologies independently contribute to brain structural degradation and cognitive decline.[2–9] Autopsy studies, for example, reported patients with AD and cerebrovascular disease to show lower AD burden than those without cerebrovascular disease given the same dementia severity.[7,8] Correspondingly, neuroimaging studies have demonstrated that Aβ and cerebrovascular disease affected structural network disruption and cortical thinning in distinct brain areas, and contributed to declines in corresponding cognitive domains in cognitively impaired patients.[2,4,9] However, little remains known about the effect of co-occurring AD and cerebrovascular disease pathologies on brain functional network changes.

Intrinsic functional connectivity (FC), which measures the temporal synchrony between low-frequency oscillations in blood oxygenation level–dependent fMRI signals under task-free conditions, offers a promising tool for the understanding of disease-related changes in brain functional networks. Using such methods, studies have similarly demonstrated differential effects of AD and cerebrovascular disease pathologies on FC. AD, on its own, is prominently associated with disruptions in the default mode network (DMN),[10–12] a network linked to autobiographical and episodic memory retrieval.[13] Patients with AD have consistently shown reduced DMN FC compared to healthy controls.[10–12] Importantly, DMN disruptions are apparent at prodromal AD stages, with cross-sectional studies reporting both increases and decreases in DMN FC of patients with mild cognitive impairment (MCI)[14–16] as well as cognitively normal elderly with significant Aβ burden.[17,18] Increased Aβ burden was also associated with reduced whole-brain FC to the posterior cingulate cortex (a key DMN region) in a cross-sectional cohort comprising healthy participants and those with MCI.[19] Cerebrovascular disease, on the other hand, is primarily associated with disruptions in the executive control network (ECN),

a frontoparietal network associated with executive function. Studies have linked cerebrovascular disease to declines in executive function,[20] reduced frontal lobe metabolism,[21] and disrupted FC in frontoparietal regions.[22,23]

While few studies have examined FC changes in patients with co-occurring AD and cerebrovascular disease pathologies, there is some cross-sectional evidence supporting the presence of such divergent FC effects in these patients. In one study, patients with Aβ-positive AD and patients with Aβ-negative subcortical vascular dementia showed disease-specific vulnerability in DMN FC (i.e., reduced posterior FC in AD, reduced frontal FC in subcortical vascular dementia), while patients with subcortical vascular dementia showed declines in ECN FC. Further, patients with mixed dementia (Aβ-positive subcortical vascular dementia) exhibited greater disruptions in DMN and ECN FC compared to patients with AD and patients with subcortical vascular dementia.[24] In another study, patients with AD without cerebrovascular disease exhibited reduced DMN FC compared to those with cerebrovascular disease, while patients with AD and cerebrovascular disease showed increased frontal ECN FC compared to those without cerebrovascular disease. These changes in the ECN were also mirrored in patients with cognitive impairment but no dementia with and without cerebrovascular disease, indicating that the divergent FC changes were present even at early disease stages.[25]

However, while these studies provide insight on the differential FC effects of AD and cerebrovascular disease in cross-sectional cohorts, the influence of AD and cerebrovascular disease pathologies on the longitudinal trajectory of FC changes in patients with MCI remains unknown. Our study thus sought to examine the effects of baseline Aβ and cerebrovascular disease markers on longitudinal functional network changes in patients with amnestic MCI (aMCI) and patients with subcortical vascular MCI (svMCI), which are often regarded as prodromal stages of AD and subcortical vascular dementia, respectively. Specifically, we focused on FC changes in the DMN and ECN, 2 key networks implicated in AD and cerebrovascular disease. Given past evidence, we hypothesized that the 2 MCI subtypes with and without Aβ burden would exhibit divergent FC changes over time. Aβ burden, as measured by Pittsburgh compound B (PiB) standardized uptake value ratio (SUVR), would be associated with longitudinal DMN FC declines. Conversely, cerebrovascular burden, as measured by lacune number, would be primarily associated with longitudinal ECN FC changes.

Methods

Participants

We prospectively recruited 105 patients with MCI from September 2008 to September 2011 at Samsung Medical Center in Seoul, South Korea. Diagnoses of MCI were made using Petersen criteria,[26] with the following modifications[27]: (1) subjective cognitive complaint by patients or caregivers; (2) normal activities of daily living (ADL) determined clinically and according to the instrumental ADL scale[28]; (3) objective cognitive impairment below the 16th percentile (i.e., below 1 SD) of education- and age-matched norms in at least one of 4 domains (memory, visuospatial, language, or frontal-executive function) of the Seoul Neuropsychological Screening Battery (SNSB)[29]; and (4) no dementia.

Patients were further diagnosed with svMCI if they had subcortical vascular features defined as significant ischemia on MRI and focal neurologic symptoms or signs such as corticobulbar signs, pyramidal signs, or parkinsonism.[30] Significant ischemia was defined as severe white matter hyperintensities on fluid-attenuated inversion recovery (FLAIR) images meeting the following criteria: (1) white matter hyperintensities ≥10 mm in the periventricular white matter and (2) white matter hyperintensities ≥25 mm in the deep white matter, which is consistent with an extensive or diffusely confluent lesion. Patients were further diagnosed with aMCI if they showed objective impairment below the 16th percentile of education- and age-matched norms on either the visual or verbal memory domain of the SNSB and did not have significant ischemia on MRI.

Patients were evaluated by clinical interviews and neuropsychological and neurologic examinations at baseline. All patients underwent laboratory tests including a complete blood count, syphilis serology, vitamin B_{12}/folate, blood chemistry, and thyroid function tests. Absence of structural lesions including brain tumors, vascular malformation, territorial cerebral infarction. and hippocampal sclerosis was confirmed using MRI. Patients in this cohort were followed up annually with neuropsychological tests and brain MRI scans for up to 4 years. In total, there were 91 patients (33 aMCI and 58 svMCI) who had at least 2 timepoints of brain MRI (aMCI: 29 with 2 timepoints, 4 with 3 timepoints; svMCI: 10 with 2 timepoints, 14 with 3 timepoints, 34 with 4 timepoints).

Standard protocol approvals, registrations, and patient consents

The study protocol was approved by the Institutional Review Board of Samsung Medical Center, and written informed consent was obtained from all patients.

Image acquisition

MRI acquisition

We acquired standardized T2-weighted, T1-weighted, FLAIR, and task-free fMRI from patients at Samsung Medical Center using a Philips Achieva 3.0 T MRI scanner (Philips Healthcare, Best, the Netherlands). Imaging measures for the MRI were as follows: (1) T1-weighted: repetition time =

9.9 ms, echo time = 4.6 ms, flip angle = 8°, voxel resolution = 0.5 mm^3 isotropic, matrix size = 240 × 240 pixels, reconstructed to 480 × 480 over a field of view of 240 mm; (2) T2-weighted: axial slice thickness = 5.0 mm, interslice thickness = 1.5 mm, repetition time = 3,000 ms, echo time = 80 ms, flip angle = 90°, and matrix size = 512 × 512 pixels; (3) FLAIR: axial slice thickness = 2 mm, no gap, repetition time = 11,000 ms, echo time = 125 ms, flip angle = 90°, and matrix size = 512 × 512 pixels; and (4) task-free fMRI: echoplanar imaging sequence (5 minutes, 100 volumes), repetition time = 3,000 ms, echo time = 35 ms, flip angle = 90°, and voxel resolution = 1.7 × 1.7 × 4 mm^3. During the fMRI scan, participants were instructed to fixate on a centrally located white crosshair against a black background.

[^{11}C]PiB-PET acquisition

At baseline, all patients underwent [^{11}C]PiB-PET scans at Asan Medical Center or Samsung Medical Center using a Discovery STe PET/CT scanner (GE Medical Systems, Milwaukee, WI) (3D scanning mode, whole brain, 35 slices with thickness of 4.25 mm). [^{11}C]PiB was first injected as a bolus with a mean dose of 420 MBq (range 259–550 MBq). A CT scan was then performed for attenuation correction 60 minutes after injection, followed by a 30-minute emission static PET scan. We reconstructed attenuation-corrected PET images from the CT data using an iterative reconstruction method following previous approach.[31]

Image processing

[^{11}C]PiB-PET data analysis

PiB-PET images were first coregistered to the corresponding T1-weighted images, and subsequently normalized to Montreal Neurological Institute (MNI) 152 (MNI152) standard space. Regional values of PiB retention on the normalized PiB images were then obtained using an automated volume-of-interest (VOI) analysis. Following previous protocol,[2,32,33] 28 cortical VOIs were selected from the automated anatomical labeling atlas[34] and comprised the bilateral frontal, parietal, lateral temporal, occipital, and posterior cingulate cortex. We computed regional SUVRs by dividing each VOI uptake ratio by the mean uptake of the cerebellar cortex (cerebellum crus1 and crus2) (reference region). To obtain a measure of Aβ burden, global PiB SUVR was calculated as the volume-weighted average uptake ratio of the above 28 VOIs. Patients were categorized into PiB-positive (PiB+) or PiB-negative (PiB−) using a global PiB SUVR cutoff value of 1.5.[31]

Assessment of lacune number

We defined lacunes as small lesions (≤15 mm and ≥3 mm in diameter) with high signal on T2-weighted images, low signal on T1-weighted images, and a perilesional halo on FLAIR images according to Standards for Reporting Vascular Changes on Neuroimaging (STRIVE) criteria.[35] The number of lacunes was manually counted by 2 neurologists (κ value = 0.78).

Functional imaging

Preprocessing of task-free fMRI was performed using the Analysis of Functional NeuroImages software[36] and FMRIB Software Library[37] in accordance with previous protocol.[25] The preprocessing procedure involved the following: (1) discarding of first 5 volumes for magnetic field stabilization; (2) slice-time and motion correction; (3) time series despiking; (4) grand mean scaling; (5) spatial smoothing using a 6-mm full-width at half-maximum Gaussian kernel; (6) bandpass temporal filtering at 0.009–0.1 Hz; (7) removal of linear and quadratic trends; (8) coregistration to T1-weighted images using boundary-based registration and subsequently nonlinear registration of fMRI to MNI152 space; and (9) regression of global signal, white matter, CSF, and 6 motion parameters from the preprocessed fMRI.

Structural imaging

Gray matter volume (GMV) probability maps at each timepoint were obtained from structural images using a longitudinal voxel-based morphometry protocol following previous work.[38] This protocol used the VBM8 toolbox (Structural Brain Mapping Group; dbm.neuro.uni-jena.de/software/) in Statistical Parametric Mapping (SPM12; Wellcome Trust Centre for Neuroimaging; fil.ion.ucl.ac.uk/spm/software/spm12/) and included (1) realignment of intraparticipant images across timepoints; (2) creation of participant-specific mean reference images; (3) intraparticipant signal inhomogeneity correction using the reference image; (4) segmentation into gray matter, white matter, and CSF using the adaptive Maximum A Posterior method, which does not require a priori information about tissue probabilities; (5) creation of a customized template using nonlinear diffeomorphic anatomical registration through exponentiated lie algebra (DARTEL) registration of the affine-registered segmented images; (6) registration of reference GMV and white matter volume probability maps to the customized template in standard MNI152 space; (7) application of registration in step 6 to individual GMV and white matter volume probability maps at each timepoint; and (8) nonlinear modulation of preprocessed images by multiplying voxels with the nonlinear component of the Jacobian determinant to correct for individual brain sizes.

Derivation of FC matrices and mean nodal GMV

DMN and ECN FC matrices were generated separately for each participant at each timepoint. To obtain these FC matrices, we first identified regions of interest (nodes) pertaining to the DMN (18 nodes) and ECN (22 nodes) based on a previous FC-based parcellation scheme[39] (full list of nodes are provided in table e-1, doi.org/10.5061/dryad.v5h2fd7). The average time series of each node was then extracted from each participant's preprocessed fMRI in standard space. To generate the network-specific FC matrices (DMN: 153 [= (18 × 17)/2] connections; ECN: 231 [= (22 × 21)/2] connections), Pearson correlation was computed between the mean time series of each pair of nodes within each network (edges) and converted to z scores using Fisher r-to-z transformation.

To obtain participant-specific mean GMV for each node, GMV probability values from individual GMV maps were averaged across all voxels within each node.

Statistical analyses

From the dataset of 91 patients with at least 2 timepoints of MRI data, we further excluded those whose data failed the motion criteria (maximum absolute displacement <3 mm, maximum relative displacement <1 mm). This gave rise to a subset of 85 patients (30 aMCI [14 PiB−, 16 PiB+] [26 with 2 timepoints, 4 with 3 timepoints] and 55 svMCI [37 PiB−, 18 PiB+] [13 with 2 timepoints, 16 with 3 timepoints, 26 with 4 timepoints]) whose data were used for further statistical analyses (table 1). As age and education differed between the groups, these variables were added as nuisance covariates in all analyses.

Effect of time on brain FC

Linear mixed effects models were used to examine longitudinal FC changes for each group (aMCI PiB−, aMCI PiB+, svMCI PiB−, svMCI PiB+) separately. Analyses were performed using the lme4[40] package in R 3.0.3[41] with Rstudio.[42] In these 4 separate models, time (i.e., number of years from baseline) was modeled as a random effect (random intercepts and slopes) for each participant, while baseline age, sex, and years of education were modeled as fixed effects. The linear mixed model for the effects of time on FC is as follows:

$$Y_{ij} = \gamma_{00} + \gamma_{01}(Sex_j) + \gamma_{02}(Education_j) + \gamma_{03}(Age_j) + \gamma_{10}(Time_{ij}) + \mu_{0j} + \mu_{1j}(Time_{ij}) + r_{ij} \quad (1)$$

where Y_{ij} denotes the edgewise FC for each participant j at timepoint i, γs denote the estimated fixed effect coefficients, μs denote the estimated random effect coefficients, and r_{ij} denotes the residual for each participant j at timepoint i.

Difference in effect of time on FC between aMCI PiB+ and svMCI PiB− patients

To further test our hypothesis of divergent effects of Aβ and cerebrovascular disease burden on FC, we in addition examined differences in the effect of time on FC between the 2 groups who likely did not have mixed pathology—aMCI PiB+ and svMCI PiB−. The model included time as random effect, and group (aMCI PiB + vs svMCI PiB−), baseline age, sex, and education as fixed effects. In addition, the effect of time was allowed to vary as a function of group (i.e., group by time interaction). The linear mixed model is thus:

$$Y_{ij} = \gamma_{00} + \gamma_{01}(Sex_j) + \gamma_{02}(Education_j) + \gamma_{03}(Age_j) + \gamma_{04}(Group_j) + \gamma_{10}(Time_{ij}) + \gamma_{11}(Group_j * Time_{ij}) + \mu_{0j} + \mu_{1j}(Time_{ij}) + r_{ij} \quad (2)$$

where Y_{ij} denotes the edgewise FC for each participant j at timepoint i, γs denote the estimated fixed effect coefficients, μs denote the estimated random effect coefficients, and r_{ij} denotes the residual for each participant j at timepoint i.

Effect of baseline PiB SUVR and lacune number on longitudinal changes in FC

Finally, instead of separating individuals into PiB+ and PiB− groups, we examined the effects of baseline PiB SUVR and lacune number as continuous variables on longitudinal edgewise FC changes. PiB SUVR and lacune numbers were log-transformed as they had skewed distributions. Separate

Table 1 Participant demographic and clinical characteristics at baseline

	aMCI PiB− (n = 14)	aMCI PiB+ (n = 16)	svMCI PiB− (n = 37)	svMCI PiB+ (n = 18)	*p* Value
Age, y	71.93 (6.42)	68.38 (8.45)[d]	72.22 (7.14)	77.61 (5.72)[b]	0.003[e]
Male/female	7/7	8/8	11/26	9/9	0.315
Education, y	11.14 (6.41)	12.81 (2.79)[c]	7.97 (4.64)[b]	10.58 (5.52)	0.008[e]
MMSE	26.50 (2.18)	25.88 (2.03)	26.08 (2.25)	25.78 (4.10)	0.886
CDR	0.46 (0.13)	0.50 (0.00)	0.47 (0.11)	0.47 (0.12)	0.793
PiB SUVR	1.29 (0.13)[b,d]	2.18 (0.36)[a,c]	1.27 (0.11)[b,d]	1.99 (0.34)[a,c]	<0.001[e]
Lacune number	1.43 (3.72)[c,d]	0.25 (0.68)[c,d]	6.84 (7.31)[a,b]	4.28 (4.32)[a,b]	<0.001[e]
Conversion to dementia, n (%)	4 (28.6)	10 (62.5)[c]	4 (10.8)[b,d]	7 (38.9)[c]	0.001[e]
Time to conversion, y	3.25 (0.50)[d]	2.60 (0.52)[d]	2.75 (1.71)[d]	1.43 (0.79)[a–c]	0.012[e]

Abbreviations: aMCI = amnestic mild cognitive impairment; CDR = Clinical Dementia Rating; MMSE = Mini-Mental State Examination; PiB = Pittsburgh compound B; SUVR = standardized uptake value ratio; svMCI = subcortical vascular mild cognitive impairment.
Values are mean (SD) unless indicated otherwise.
[a] Represents a significant difference from the aMCI PiB− group.
[b] Represents a significant difference from the aMCI PiB+ group.
[c] Represents a significant difference from the svMCI PiB− group.
[d] Represents a significant difference from the svMCI PiB+ group.
[e] Indicates a significant difference between groups ($p < 0.05$).

linear mixed models were performed for patients with svMCI, aMCI, and across all patients. In these 3 models, we modeled time as random effect, and sex, education, age, baseline PiB SUVR, and baseline lacune number as fixed effects, as follows:

$$Y_{ij} = \gamma_{00} + \gamma_{01}(Sex_j) + \gamma_{02}(Education_j) + \gamma_{03}(Age_j) + \gamma_{04}(PiB\ SUVR_j) + \gamma_{05}(Lacune_j) + \gamma_{10}(Time_{ij}) + \gamma_{11}(PiB\ SUVR_j{*}Time_{ij}) + \gamma_{12}(Lacune_j{*}Time_{ij}) + \mu_{0j} + \mu_{1j}(Time_{ij}) + r_{ij} \quad (3)$$

where Y_{ij} denotes the edgewise FC for each participant j at timepoint i, γs denote the estimated fixed effect coefficients, μs denote the estimated random effect coefficients, and r_{ij} denotes the residual for each participant j at timepoint i.

For all statistical analyses, both uncorrected ($p < 0.005$) and multiple comparisons corrected (false discovery rate–adjusted $p < 0.05$) results were reported. In addition, to determine if GMV changes or conversion status accounted for the observed findings, we repeated the above analyses with mean nodal GMV or conversion status included as covariates (e-Methods, doi.org/10.5061/dryad.v5h2fd7).

Data availability

The data that support the findings of this study are available upon request from the corresponding authors (J.Z. and S.W.S.). The data are not publicly available due to institute policy.

Results

Effect of Aβ burden on longitudinal DMN and ECN FC changes

We first examined longitudinal FC changes for each of the 4 groups separately. In PiB+ groups (i.e., aMCI PiB+ and svMCI PiB+), DMN FC was found to decrease with time. In contrast, PiB− groups (i.e., svMCI PiB− and aMCI PiB−) showed predominantly DMN FC increases with time (figure 1A and table e-2, doi.org/10.5061/dryad.v5h2fd7). Our findings thus suggest that high Aβ burden is associated with longitudinal declines in DMN FC, with some longitudinal DMN FC increases at low Aβ burden. To further confirm the association between high Aβ burden and longitudinal DMN FC declines, we compared differences in longitudinal FC changes between aMCI PiB+ (representing patients with only Aβ pathology) and svMCI PiB+ (representing patients with only cerebrovascular pathology). Consistent with our earlier findings, aMCI PiB+ patients showed steeper longitudinal declines in DMN FC compared to svMCI PiB− patients (figure 2A and table e-4, doi.org/10.5061/dryad.v5h2fd7).

Examination of the influence of baseline PiB SUVR as continuous variable on longitudinal FC (in aMCI and svMCI groups separately as well as across all patients) similarly revealed a relationship between higher Aβ burden and longitudinal DMN FC declines. Specifically, we found negative PiB SUVR × time effects on DMN FC in both patients with aMCI and patients with svMCI (figure 3A and table e-6, doi.org/10.5061/dryad.v5h2fd7). Visualization of the changes in DMN FC as a function of PiB SUVR in patients with svMCI revealed an inverted U-shape relationship between longitudinal DMN FC changes and baseline PiB SUVR: low baseline PiB SUVR values were associated with mainly longitudinal DMN FC increases, while high baseline PiB SUVR values were associated with longitudinal DMN FC declines (figure e-1, doi.org/10.5061/dryad.v5h2fd7). Across all patients, baseline PiB SUVR similarly showed an inverted U-shape relationship (negative PiB SUVR × time effect) with longitudinal DMN FC changes (figure 4A and figure e-2, doi.org/10.5061/dryad.v5h2fd7).

As for the relationship between PiB SUVR and longitudinal ECN FC changes, we found that baseline PiB SUVR was associated with longitudinal ECN FC changes of only one edge in patients with aMCI (figure 3C), but not in patients with svMCI or across all patients (table e-6, doi.org/10.5061/dryad.v5h2fd7). Collectively, our findings indicate a link between high Aβ burden and longitudinal declines in DMN FC, with an initial increase in DMN FC over time when Aβ burden levels are low.

Effect of cerebrovascular disease burden on longitudinal DMN and ECN FC changes

By comparison, while aMCI (i.e., aMCI PiB− and aMCI PiB+) groups showed a mixture of longitudinal ECN FC increases and decreases, svMCI (i.e., svMCI PiB− and svMCI PiB+) groups showed only ECN FC increases with time, indicating that high cerebrovascular burden is associated with longitudinal ECN FC increases (figure 1B and table e-2, doi.org/10.5061/dryad.v5h2fd7). Direct comparisons between aMCI PiB+ and svMCI PiB− patients further confirmed this relationship, with svMCI PiB− patients showing steeper longitudinal increases in ECN FC compared to aMCI PiB+ patients (figure 2B and table e-4, doi.org/10.5061/dryad.v5h2fd7).

When examining the effect of baseline lacune numbers as continuous variables on longitudinal FC changes, we similarly found greater number of lacunes to be associated with greater longitudinal ECN FC changes. Specifically, we found lacune × time effects on ECN FC in a number of edges in patients with svMCI but not in patients with aMCI (figure 3D and table e-6, doi.org/10.5061/dryad.v5h2fd7). Most of these edges showed longitudinal ECN FC increases at low lacune numbers and longitudinal ECN FC decreases at high lacune numbers (i.e., positive effect, inverted U-shape relationship), while one edge showed longitudinal ECN FC declines at low lacune numbers and longitudinal ECN FC increases at high lacune numbers (i.e., negative effect, U-shape relationship) (figure e-1B, doi.org/10.5061/dryad.v5h2fd7). Across all patients, baseline lacune numbers also showed an inverted U-shape relationship (negative lacune × time effect) with

Figure 1 Longitudinal default mode network (DMN) and executive control network (ECN) functional connectivity (FC) changes in each group

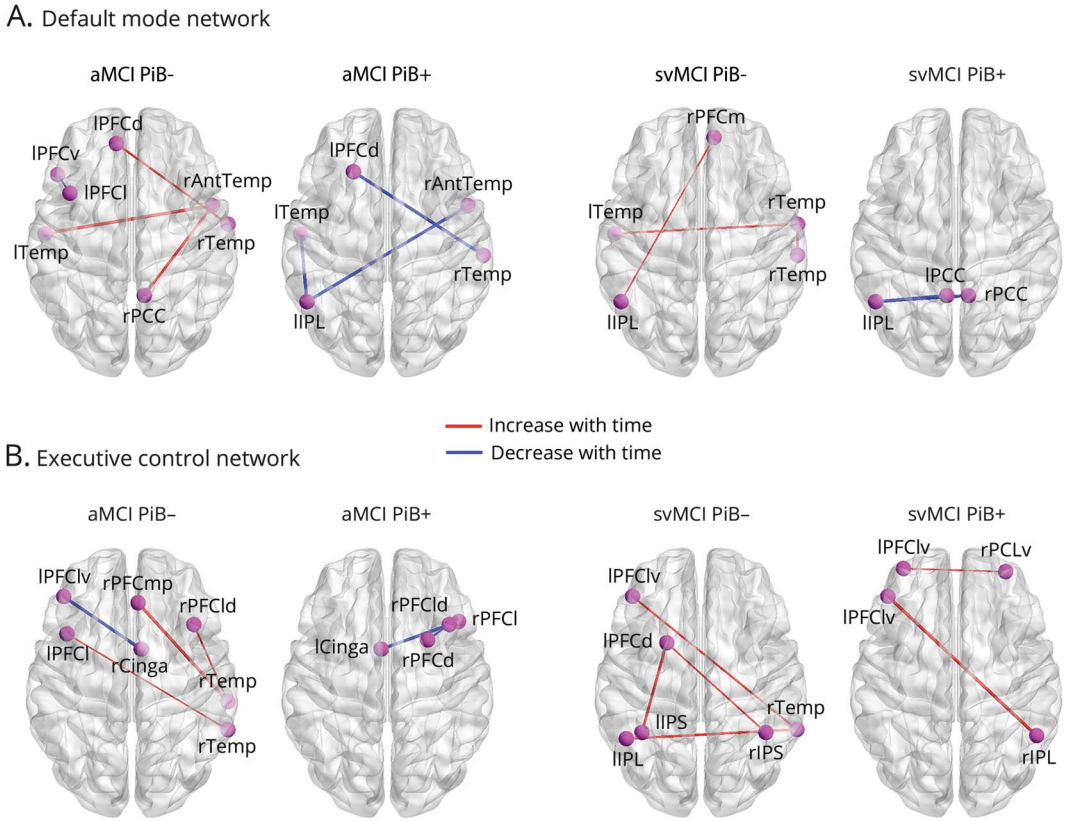

Brain maps display edges that show significant longitudinal FC changes for each group. Red lines indicate increases in FC over time, while blue lines indicate decreases in FC over time. Edges displayed are thresholded at $p < 0.005$ (uncorrected) (edges passing false discovery rate–corrected threshold of $p < 0.05$ are highlighted in bold in table e-2, doi.org/10.5061/dryad.v5h2fd7). (A) In the DMN, Pittsburgh compound B (PiB)+ (i.e., amnestic mild cognitive impairment [aMCI] PiB+ and subcortical vascular mild cognitive impairment [svMCI] PiB+) patients exhibited longitudinal FC declines, while PiB− (i.e., aMCI PiB− and svMCI PiB−) patients exhibited predominantly longitudinal FC increases. (B) In the ECN, svMCI (PiB− and PiB+) patients showed longitudinal FC increases. By comparison, aMCI PiB− patients exhibited both longitudinal FC increases and decreases, while aMCI PiB+ patients exhibited longitudinal FC declines. AntTemp = anterior temporal cortex; Cinga = anterior cingulate sulcus; IPL = inferior parietal lobule; IPS = intraparietal sulcus; l = left hemisphere; PCC = posterior cingulate cortex; PFCd = dorsal prefrontal cortex; PFCl = lateral prefrontal cortex; PFCld = lateral dorsal prefrontal cortex; PFClv = lateral ventral prefrontal cortex; PFCm = medial prefrontal cortex; PFCmp = medial posterior prefrontal cortex; PFCv = ventral prefrontal cortex; r = right hemisphere; temp = temporal cortex.

longitudinal ECN FC changes (figure 4B and figure e-2, doi.org/10.5061/dryad.v5h2fd7).

In regards to the association between baseline lacune numbers and longitudinal DMN FC changes, there was only one negative lacune × time effect on DMN FC in patients with svMCI (figure 3B), but no association in patients with aMCI and across all patients (table e-6, doi.org/10.5061/dryad.v5h2fd7). Together, the findings indicate that high cerebrovascular burden is associated predominantly with longitudinal changes in ECN FC.

Validation analyses

For all analyses, similar findings were obtained even after controlling for GMV or conversion status, suggesting that the effects of Aβ and cerebrovascular disease burden on longitudinal DMN and ECN FC changes are unlikely due to changes in GMV or conversion status (tables e-2 to e-7, doi.org/10.5061/dryad.v5h2fd7).

Discussion

We sought to examine the effects of Aβ and cerebrovascular disease burden on longitudinal changes in DMN and ECN FC of patients with MCI. We showed that Aβ burden was associated with longitudinal DMN FC declines, while cerebrovascular disease burden was associated with longitudinal ECN FC changes. Specifically, PiB+ patients showed longitudinal DMN FC declines, while patients with svMCI showed longitudinal ECN FC increases. Direct comparisons between aMCI PiB+ and svMCI PiB− patients revealed the same divergent pattern: aMCI PiB+ patients had steeper longitudinal declines in DMN FC compared to svMCI PiB− patients, while svMCI PiB− patients had steeper longitudinal increases in ECN FC compared to aMCI PiB+ patients. Finally, using baseline PiB SUVR and lacune numbers as continuous variables, baseline PiB SUVR showed an inverse U-shape relationship with longitudinal DMN FC changes in both aMCI and svMCI, while baseline lacune numbers showed both

Figure 2 Differences in longitudinal default mode network (DMN) and executive control network (ECN) functional connectivity (FC) changes between amnestic mild cognitive impairment (aMCI) Pittsburgh compound B (PiB)+ and subcortical vascular mild cognitive impairment (svMCI) PiB− patients

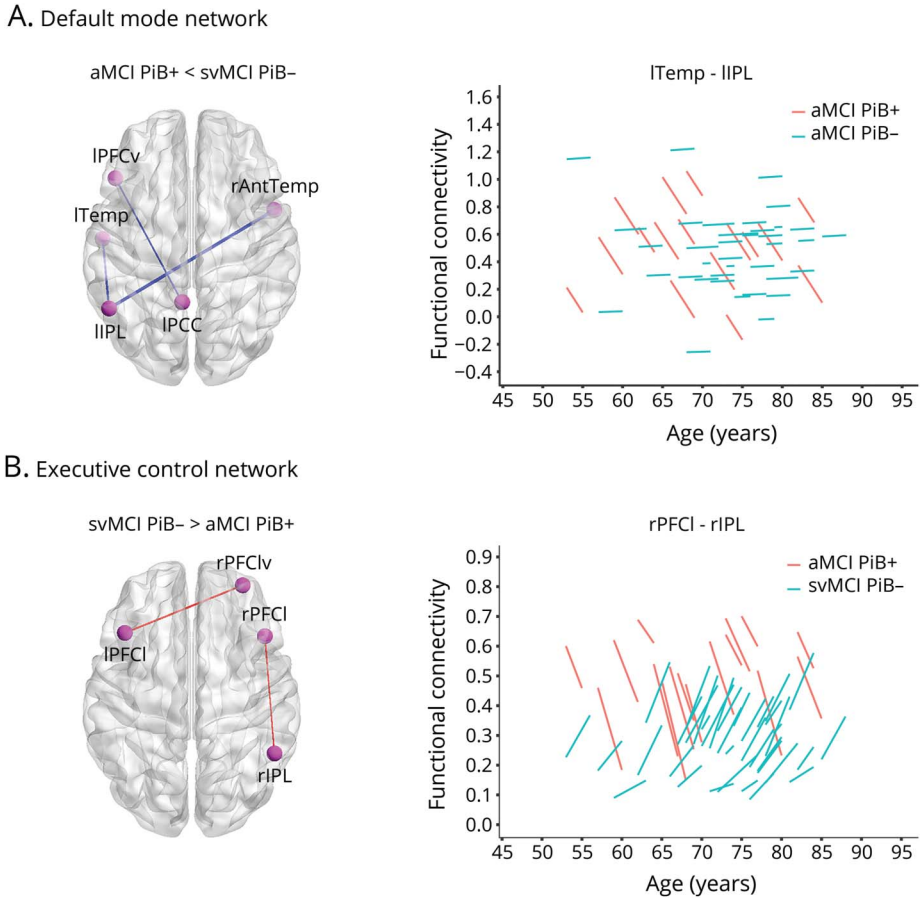

Brain maps display edges that show significant differences in FC changes over time between aMCI PiB+ and svMCI PiB− patients. Spaghetti plots indicate individual model-fitted longitudinal changes in FC of representative edges for each network. Edges displayed are thresholded at $p < 0.005$ (uncorrected). (A) aMCI PiB+ patients showed greater longitudinal declines in DMN FC compared to svMCI PiB− patients. (B) In contrast, svMCI PiB− patients showed greater longitudinal increases in ECN FC compared to aMCI PiB+ patients. AntTemp = anterior temporal cortex; IPL = inferior parietal lobule; l = left hemisphere; PCC = posterior cingulate cortex; PFCl = lateral prefrontal cortex; PFClv = lateral ventral prefrontal cortex; PFCv = ventral prefrontal cortex; r = right hemisphere; temp = temporal cortex.

U-shape and inverse U-shape relationships with longitudinal ECN FC changes in patients with svMCI. Taken together, our longitudinal findings extend previous cross-sectional findings and support the divergent effects of Aβ and cerebrovascular burden on DMN and ECN FC, respectively.

Aβ burden is associated with longitudinal DMN FC declines in both aMCI and svMCI

Consistent with previous evidence supporting DMN involvement at prodromal stages of AD,[17,18] we showed that Aβ burden was associated with longitudinal DMN FC decreases in MCI. Both aMCI PiB+ and svMCI PiB+ patients showed decreased DMN FC with time, with aMCI PiB+ patients showing greater longitudinal DMN FC declines than svMCI PiB− patients. By comparison, both aMCI PiB− and svMCI PiB− patients showed predominantly longitudinal DMN FC increases. Further, baseline PiB SUVR showed inverted U-shape relationships with longitudinal DMN FC changes (i.e., longitudinal FC increases at low PiB SUVR, longitudinal FC decreases at high PiB SUVR) in aMCI and svMCI separately and across all patients. This observed inverted U-shape association between baseline PiB SUVR and DMN FC changes is consistent with studies showing that Aβ is associated with initial hyperconnectivity followed by subsequent hypoconnectivity in the DMN of preclinical and prodromal AD.[43,44] One possible account for this hyperconnectivity/hypoconnectivity phenomenon is that the early presence of soluble Aβ oligomers (undetectable by Aβ PET imaging) prior to the formation of Aβ plaques induces initial abnormal hyperactivity, with silencing of brain circuits only occurring at later disease stages.[45] Alternatively, the initial FC increase could represent compensatory increases in use of neural resources to cope with the early neuronal injury. As Aβ burden continues to increase, FC eventually declines when neural resource loss reaches a threshold and increased FC is no longer a viable response to the insult.[46] Further, tau has recently been proposed to moderate the relationship between Aβ burden and FC changes.[44] Future studies examining the effects of both tau and Aβ on FC might shed more light on the factors contributing to the hyperconnectivity/hypoconnectivity phenomena in early AD.

While Aβ burden was observed to be associated with longitudinal ECN FC declines in aMCI as well, the effects were less

Figure 3 Effects of baseline lacune number and Pittsburgh compound B (PiB) standardized uptake value ratio (SUVR) on longitudinal functional connectivity (FC) changes in subcortical vascular mild cognitive impairment (svMCI) and amnestic mild cognitive impairment (aMCI)

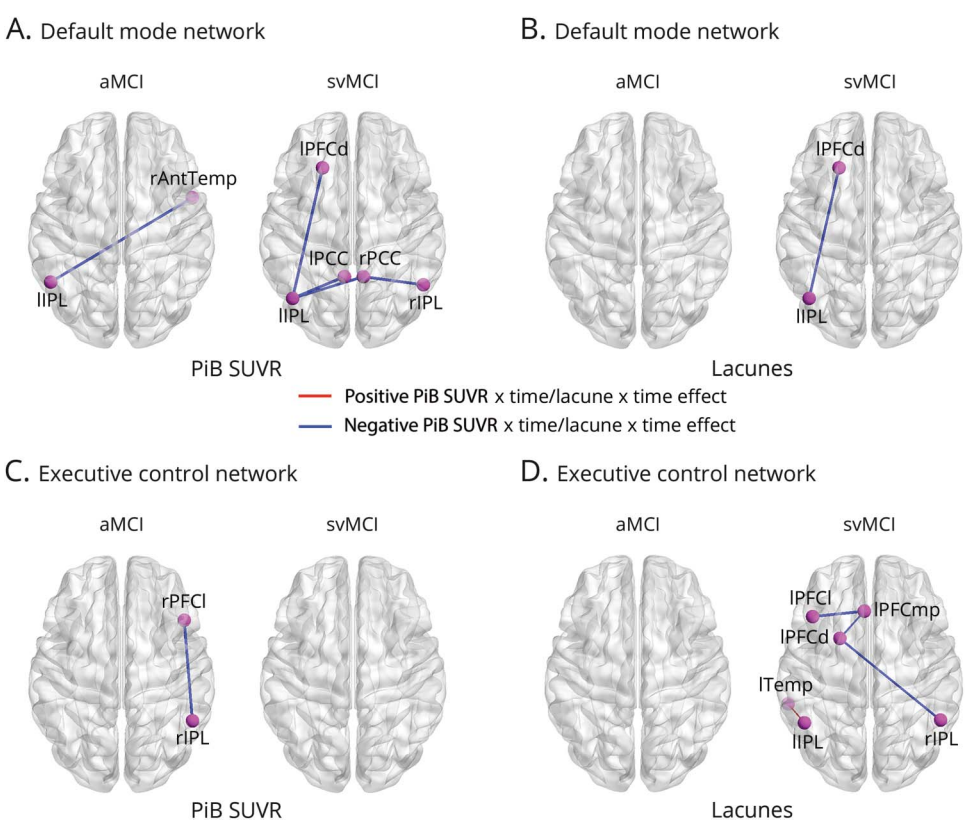

Brain maps display edges that show significant effects of lacune × time or PiB SUVR × time on FC in svMCI and aMCI. Red lines indicate positive lacune × time or PIB SUVR × time effects, while blue lines indicate negative lacune × time or PiB SUVR × time effects. Edges displayed are thresholded at $p < 0.005$ (uncorrected) (edges passing false discovery rate corrected threshold of $p < 0.05$ are highlighted in bold in table e-6, doi.org/10.5061/dryad.v5h2fd7). (A) Both aMCI and svMCI showed negative PiB SUVR × time effects on default mode network (DMN) connectivity in several edges, indicating that longitudinal changes in DMN FC became more negative/less positive as baseline PiB SUVR increases in both subtypes. (C) On the other hand, only patients with aMCI showed a negative PiB SUVR × time effect on executive control network (ECN) FC in one edge. By comparison, patients with svMCI showed (B) a negative lacune × time effect on DMN FC in one edge, and (D) both negative and positive lacune × time effects on ECN FC in several edges. No lacune × time effects were observed for patients with aMCI. AntTemp = anterior temporal cortex; IPL = inferior parietal lobule; l = left hemisphere; PCC = posterior cingulate cortex; PFCd = dorsal prefrontal cortex; PFCl = lateral prefrontal cortex; PFCmp = medial posterior prefrontal cortex; r = right hemisphere; temp = temporal cortex.

widespread, with only one edge showing a negative PiB SUVR × time effect. Moreover, there was no Aβ burden effect on longitudinal ECN FC changes in patients with svMCI. Given that svMCI PiB+ patients showed instead longitudinal ECN FC increases, it is possible that the increase in ECN FC as a result of high cerebrovascular burden in patients with svMCI predominated and masked the declines in ECN FC brought about by Aβ burden. Taken together, our findings thus support DMN disruptions as a key feature of AD and highlight its utility in tracking early AD changes.

Interestingly, we note that the spatial pattern of Aβ-related DMN FC disruptions differed between the 2 subtypes. In particular, patients with aMCI showed Aβ-related DMN FC disruptions in edges involving the temporal lobes, while patients with svMCI showed declines in edges involving the posterior cingulate cortex. These differences in spatial vulnerability patterns between the 2 subtypes might be related to differences in their Aβ distribution patterns. One study examining PiB retention in MCI subtypes showed that svMCI PiB+ patients had increased retention in occipital, precuneus, and posterior cingulate cortices, while patients with aMCI PiB+ had increased retention in striatum and temporal areas.[47] Future research could explore the relationship between Aβ distribution and FC in the 2 subtypes and examine how they might differentially affect cognition.

Cerebrovascular disease burden is associated with longitudinal changes in ECN FC regardless of Aβ status

Cerebrovascular disease burden, on the other hand, was associated with longitudinal ECN FC changes. Both svMCI PiB− and svMCI PiB+ patients showed longitudinal ECN FC increases, with svMCI PiB− patients showing steeper longitudinal ECN FC increases compared to aMCI PiB+ patients. Baseline lacune numbers also showed mostly inverted U-shape relationships with longitudinal ECN changes (i.e., longitudinal FC increases at low lacune numbers, longitudinal FC decreases at high lacune numbers) in patients with svMCI and across all patients but not patients with aMCI. The absence of an association in patients with aMCI is likely due to the low proportion of patients with aMCI with at least one lacune (aMCI: 23.3%; svMCI: 85.5%). By comparison, cerebrovascular burden effects on DMN FC were less widespread and evident only with significant cerebrovascular burden, with a negative lacune × time effect found for only one edge in patients with svMCI but not in patients with aMCI. Overall, our findings are consistent with previous

Figure 4 Effects of baseline lacune number and Pittsburgh compound B (PiB) standardized uptake value ratio (SUVR) on longitudinal functional connectivity (FC) changes across all patients

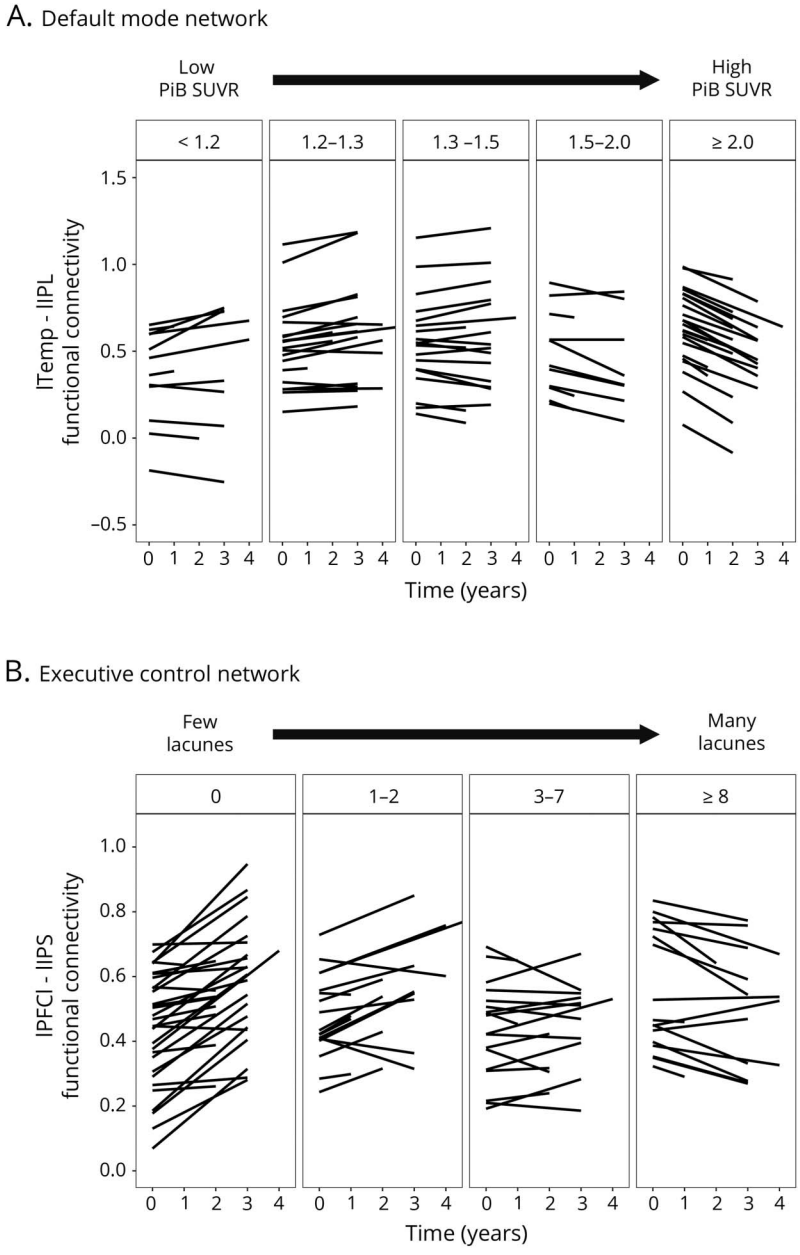

Spaghetti plots indicate individual model-fitted longitudinal changes in FC of edges showing significant lacune × time or PiB SUVR × time effects for each network across all patients ($p < 0.005$ uncorrected). Plots are distributed into bins based on PiB SUVR (5 bins) or lacune numbers (4 bins). (A) Across all patients, default mode network (DMN) FC initially increased with time at low baseline PiB SUVR values. However, this increase in DMN FC with time became less steep with increasing PiB SUVR, eventually showing sharp declines in FC at high PiB SUVR. (B) Baseline lacune numbers showed a similar inverted U relationship with longitudinal executive control network (ECN) FC changes. Baseline low lacune numbers were associated with longitudinal increases in ECN FC, while high lacune numbers were associated with longitudinal declines in ECN FC. IPL = inferior parietal lobule; IPS = intraparietal sulcus; l = left hemisphere; PFCl = lateral prefrontal cortex; temp = temporal cortex.

studies and support the link between cerebrovascular disease with frontoparietal executive dysfunctions[20] and ECN FC disruptions.[22,23,25,48]1

However, while these past studies have consistently found ECN FC disruptions, findings remain mixed in regards to whether these FC changes are increases or decreases.[22,23,25,48] In our study, we similarly found a mixture of increases and decreases in longitudinal ECN FC as a function of cerebrovascular disease burden. Several possible explanations account for these mixed changes. One possibility is that cerebrovascular-related changes in ECN FC mainly follow an inverted U-shape trajectory, akin to the hyperconnectivity/hypoconnectivity phenomena observed for Aβ burden in early AD. Initial ECN FC increases may be a compensatory mechanism to cope with cerebrovascular disease burden, with FC decreasing subsequently as increasing burden eventually results in functional network breakdown. Such compensatory mechanisms might be related to cerebrovascular disease–related changes of the underlying white matter networks. In response to ischemic injury, oligodendrocyte precursor cells can multiply and differentiate into mature oligodendrocytes to remyelinate axons[49] (resulting in compensatory FC increases), although prolonged ischemia may eventually

damage these precursor cells and result in ineffective remyelination[50] (and subsequently FC decreases). Alternatively, ECN FC increases might be aberrant. Previous studies have linked greater lacune numbers to decreased integration and increased segregation of white matter networks, which in turn related to poorer cognitive performance.[51] This increased network segregation could be due to aberrant attempts to remyelinate in response to injury, leading to greater but more inefficient local, within-network connections, and hence increased within-network FC. The structural network segregation increases may hence underlie within-network ECN FC increases, which may be accompanied by information integration loss of ECN with other networks.

Finally, the mixed findings might be due to differences in the type and location of cerebrovascular lesions across different studies. Different types of cerebrovascular lesions (e.g., lacunes, microbleeds) might have different etiologies[35,52] and hence affect FC differentially. Further, different lesion locations might be associated with decline in different cognitive functions.[53] Future studies could examine how the type and location of cerebrovascular lesions could differentially affect FC changes in prodromal and clinical dementia.

Limitations

Due to the moderate sample size (30 aMCI and 55 svMCI), we were unable to examine interaction effects between PiB SUVR and lacune number, or explore the effect of multiple variables (e.g., lesion location) on longitudinal FC changes. In addition, the follow-up period for patients was relatively short (2–4 years). As such, nonlinear longitudinal FC changes cannot be reliably tracked. Future studies with larger sample size and longer follow-up periods would allow for the examination of nonlinear trends as well as the effects of a wider range of variables (e.g., interaction effects, various pathologies) on FC in prodromal and clinical dementia. Finally, we only examined the effects of Aβ and cerebrovascular disease burden on FC within the DMN and ECN, given their key roles in AD and cerebrovascular disease, respectively. Future studies examining whole-brain FC changes could provide a more comprehensive overview of the effects of AD and cerebrovascular disease burden on functional brain networks.

We showed that Aβ and cerebrovascular disease burden had divergent effects on longitudinal DMN and ECN FC changes in both aMCI and svMCI. Specifically, Aβ burden was associated with longitudinal declines in DMN FC, while cerebrovascular disease burden was associated with longitudinal disruptions in ECN FC. Our results suggest that longitudinal changes in DMN and ECN FC reflect the underlying pathology and may be used to track early changes in AD and cerebrovascular disease.

Author contributions

J.S.X. Chong: drafting/revising the manuscript, study concept or design, analysis or interpretation of the data, accepted responsibility for conduct of research and gave final approval, and statistical analysis. H. Jang: drafting/revising the manuscript, data acquisition, analysis or interpretation of the data, and accepted responsibility for conduct of research and gave final approval. H.J. Kim: data acquisition and accepted responsibility for conduct of research and gave final approval. K.K. Ng: analysis or interpretation of the data, accepted responsibility for conduct of research and gave final approval, and statistical analysis. D.L. Na: data acquisition, study concept or design, and accepted responsibility for conduct of research and gave final approval. J.-H. Lee: drafting/revising the manuscript, study concept or design, and accepted responsibility for conduct of research and gave final approval. S.W. Seo: drafting/revising the manuscript, data acquisition, study concept or design, analysis or interpretation of the data, accepted responsibility for conduct of research and gave final approval, study supervision, and obtaining funding. J. Zhou: drafting/revising the manuscript, study concept or design, analysis or interpretation of the data, accepted responsibility for conduct of research and gave final approval, statistical analysis, study supervision, and obtaining funding.

Study funding

This study was supported by the National Research Foundation of Korea (NRF) grant funded by the Korean government (MSIP) (2017R1A2B2005081) awarded to SWS, the Brain Research Program through the National Research Foundation of Korea (NRF) funded by the Ministry of Science, ICT & Future Planning (2016M3C7A1913844) awarded to SWS, National Medical Research Council, Singapore (NMRC0088/2015), awarded to JZ, and Duke-NUS Medical School Signature Research Program funded by the Ministry of Health, Singapore, awarded to JZ.

Disclosure

The authors report no disclosures relevant to the manuscript. Go to Neurology.org/N for full disclosures.

Publication history

Received by *Neurology* November 26, 2018. Accepted in final form May 21, 2019.

References

1. Graham NL, Emery T, Hodges JR. Distinctive cognitive profiles in Alzheimer's disease and subcortical vascular dementia. J Neurol Neurosurg Psychiatry 2004;75:61–71.
2. Kim HJ, Yang JJ, Kwon H, et al. Relative impact of amyloid-beta, lacunes, and downstream imaging markers on cognitive trajectories. Brain 2016;139:2516–2527.
3. Vemuri P, Lesnick TG, Przybelski SA, et al. Vascular and amyloid pathologies are independent predictors of cognitive decline in normal elderly. Brain 2015;138:761–771.
4. Ye BS, Seo SW, Kim GH, et al. Amyloid burden, cerebrovascular disease, brain atrophy, and cognition in cognitively impaired patients. Alzheimer Dement 2015;11:494–503.e493.
5. Park JH, Seo SW, Kim C, et al. Effects of cerebrovascular disease and amyloid beta burden on cognition in subjects with subcortical vascular cognitive impairment. Neurobiol Aging 2014;35:254–260.
6. Attems J, Jellinger KA. The overlap between vascular disease and Alzheimer's disease: lessons from pathology. BMC Med 2014;12:206.
7. Toledo JB, Arnold SE, Raible K, et al. Contribution of cerebrovascular disease in autopsy confirmed neurodegenerative disease cases in the National Alzheimer's Coordinating Centre. Brain 2013;136:2697–2706.
8. Zekry D, Duyckaerts C, Moulias R, et al. Degenerative and vascular lesions of the brain have synergistic effects in dementia of the elderly. Acta Neuropathol 2002;103:481–487.

9. Kim HJ, Im K, Kwon H, et al. Clinical effect of white matter network disruption related to amyloid and small vessel disease. Neurology 2015;85:63–70.
10. Greicius MD, Srivastava G, Reiss AL, Menon V. Default-mode network activity distinguishes Alzheimer's disease from healthy aging: evidence from functional MRI. Proc Natl Acad Sci USA 2004;101:4637–4642.
11. Seeley WW, Crawford RK, Zhou J, Miller BL, Greicius MD. Neurodegenerative diseases target large-scale human brain networks. Neuron 2009;62:42–52.
12. Zhou J, Greicius MD, Gennatas ED, et al. Divergent network connectivity changes in behavioural variant frontotemporal dementia and Alzheimer's disease. Brain 2010; 133:1352–1367.
13. Spreng RN, Mar RA, Kim AS. The common neural basis of autobiographical memory, prospection, navigation, theory of mind, and the default mode: a quantitative meta-analysis. J Cogn Neurosci 2009;21:489–510.
14. Binnewijzend MA, Schoonheim MM, Sanz-Arigita E, et al. Resting-state fMRI changes in Alzheimer's disease and mild cognitive impairment. Neurobiol Aging 2012; 33:2018–2028.
15. Qi Z, Wu X, Wang Z, et al. Impairment and compensation coexist in amnestic MCI default mode network. Neuroimage 2010;50:48–55.
16. Zhou Y, Dougherty JH Jr, Hubner KF, Bai B, Cannon RL, Hutson RK. Abnormal connectivity in the posterior cingulate and hippocampus in early Alzheimer's disease and mild cognitive impairment. Alzheimer Dement 2008;4:265–270.
17. Sheline YI, Raichle ME, Snyder AZ, et al. Amyloid plaques disrupt resting state default mode network connectivity in cognitively normal elderly. Biol Psychiatry 2010;67: 584–587.
18. Sperling RA, Laviolette PS, O'Keefe K, et al. Amyloid deposition is associated with impaired default network function in older persons without dementia. Neuron 2009; 63:178–188.
19. Drzezga A, Becker JA, Van Dijk KR, et al. Neuronal dysfunction and disconnection of cortical hubs in non-demented subjects with elevated amyloid burden. Brain 2011; 134:1635–1646.
20. Prins ND, van Dijk EJ, den Heijer T, et al. Cerebral small-vessel disease and decline in information processing speed, executive function and memory. Brain 2005;128: 2034–2041.
21. Kuczynski B, Jagust W, Chui HC, Reed B. An inverse association of cardiovascular risk and frontal lobe glucose metabolism. Neurology 2009;72:738–743.
22. Schaefer A, Quinque EM, Kipping JA, et al. Early small vessel disease affects frontoparietal and cerebellar hubs in close correlation with clinical symptoms: a resting-state fMRI study. J Cereb Blood flow Metab 2014;34:1091–1095.
23. Zhang D, Liu B, Chen J, et al. Determination of vascular dementia brain in distinct frequency bands with whole brain functional connectivity patterns. PLoS One 2013;8: e54512.
24. Kim HJ, Cha J, Lee JM, et al. Distinctive resting state network disruptions among Alzheimer's disease, subcortical vascular dementia, and mixed dementia patients. J Alzheimer Dis 2015;50:709–718.
25. Chong JSX, Liu S, Loke YM, et al. Influence of cerebrovascular disease on brain networks in prodromal and clinical Alzheimer's disease. Brain 2017;140:3012–3022.
26. Petersen RC, Smith GE, Waring SC, Ivnik RJ, Tangalos EG, Kokmen E. Mild cognitive impairment: clinical characterization and outcome. Arch Neurol 1999;56:303–308.
27. Seo SW, Cho SS, Park A, Chin J, Na DL. Subcortical vascular versus amnestic mild cognitive impairment: comparison of cerebral glucose metabolism. J Neuroimaging 2009;19:213–219.
28. Ku HM, Kim JH, Kwon EJ, et al. A study on the reliability and validity of Seoul-instrumental activities of daily living (S-IADL). J Korean Neuropsychiatr Assoc 2004; 43:189–199.
29. Ahn HJ, Chin J, Park A, et al. Seoul Neuropsychological Screening Battery-dementia version (SNSB-D): a useful tool for assessing and monitoring cognitive impairments in dementia patients. J Korean Med Sci 2010;25:1071–1076.
30. Kim SH, Seo SW, Go SM, et al. Pyramidal and extrapyramidal scale (PEPS): a new scale for the assessment of motor impairment in vascular cognitive impairment associated with small vessel disease. Clin Neurol Neurosurg 2011; 113:181–187.
31. Lee JH, Kim SH, Kim GH, et al. Identification of pure subcortical vascular dementia using ^{11}C-Pittsburgh compound B. Neurology 2011;77:18–25.
32. Lee MJ, Seo SW, Na DL, et al. Synergistic effects of ischemia and beta-amyloid burden on cognitive decline in patients with subcortical vascular mild cognitive impairment. JAMA Psychiatry 2014;71:412–422.
33. Noh Y, Seo SW, Jeon S, et al. White matter hyperintensities are associated with amyloid burden in APOE4 non-carriers. J Alzheimer Dis 2014;40:877–886.
34. Tzourio-Mazoyer N, Landeau B, Papathanassiou D, et al. Automated anatomical labeling of activations in SPM using a macroscopic anatomical parcellation of the MNI MRI single-subject brain. Neuroimage 2002;15:273–289.
35. Wardlaw JM, Smith EE, Biessels GJ, et al. Neuroimaging standards for research into small vessel disease and its contribution to ageing and neurodegeneration. Lancet Neurol 2013;12:822–838.
36. Cox RW. AFNI: software for analysis and visualization of functional magnetic resonance neuroimages. Comput Biomed Res 1996;29:162–173.
37. Jenkinson M, Beckmann CF, Behrens TE, Woolrich MW, Smith SM. FSL. Neuroimage 2012;62:782–790.
38. Ng KK, Lo JC, Lim JK, Chee MW, Zhou J. Reduced functional segregation between the default mode network and the executive control network in healthy older adults: a longitudinal study. Neuroimage 2016;133:321–330.
39. Yeo BT, Krienen FM, Sepulcre J, et al. The organization of the human cerebral cortex estimated by intrinsic functional connectivity. J Neurophysiol 2011;106:1125–1165.
40. Bates D, Mächler M, Bolker B, Walker S. Fitting linear mixed-effects models Usinglme4. J Stat Softw 2015;67.
41. R Core Team. R: A language and environment for statistical computing [online]. Available at: R-project.org/. Accessed July 1, 2017
42. RStudio Team. RStudio: integrated development for R [online]. Available at: rstudio.com/. Accessed July 1, 2017
43. Palmqvist S, Schöll M, Strandberg O, et al. Earliest accumulation of β-amyloid occurs within the default-mode network and concurrently affects brain connectivity. Nat Commun 2017;8:1214.
44. Schultz AP, Chhatwal JP, Hedden T, et al. Phases of hyperconnectivity and hypoconnectivity in the default mode and Salience networks track with amyloid and tau in clinically normal individuals. J Neurosci 2017;37:4323–4331.
45. Busche MA, Chen X, Henning HA, et al. Critical role of soluble amyloid-beta for early hippocampal hyperactivity in a mouse model of Alzheimer's disease. Proc Natl Acad Sci USA 2012;109:8740–8745.
46. Hillary FG, Roman CA, Venkatesan U, Rajtmajer SM, Bajo R, Castellanos ND. Hyperconnectivity is a fundamental response to neurological disruption. Neuropsychology 2015;29:59–75.
47. Noh Y, Seo SW, Kim JH, et al. Distribution of amyloid burden in PiB(+) subcortical vascular cognitive impairment compared with Alzheimer's disease. Alzheimer Dement 2013;9:P380.
48. Kim YJ, Kwon HK, Lee JM, et al. White matter microstructural changes in pure Alzheimer's disease and subcortical vascular dementia. Eur J Neurol 2015;22: 709–716.
49. Shindo A, Liang AC, Maki T, et al. Subcortical ischemic vascular disease: roles of oligodendrocyte function in experimental models of subcortical white-matter injury. J Cereb Blood Flow Metab 2016;36:187–198.
50. Kalaria RN. Cerebrovascular disease and mechanisms of cognitive impairment: evidence from clinicopathological studies in humans. Stroke 2012;43:2526–2534.
51. Kim HJ, Im K, Kwon H, et al. Effects of amyloid and small vessel disease on white matter network disruption. J Alzheimer Dis 2015;44:963–975.
52. Jellinger KA. Pathology and pathogenesis of vascular cognitive impairment-a critical update. Front Aging Neurosci 2013;5:17.
53. Biesbroek JM, Weaver NA, Biessels GJ. Lesion location and cognitive impact of cerebral small vessel disease. Clin Sci2017;131:715–728.

Amyloid and cerebrovascular burden divergently influence brain functional network changes over time

Joanna Su Xian Chong, Hyemin Jang, Hee Jin Kim, et al.

Neurology published online September 11, 2019
DOI 10.1212/WNL.0000000000008315